



Research article

An immune competent orthotopic model of endometrial cancer with metastasis

Alyssa M. Fedorko^{a,b,1}, Tae Hoon Kim^{a,1}, Russell Broaddus^c, Rosemarie Schmandt^d, Gadiseti V.R. Chandramouli^e, Hong Im Kim^a, Jae-Wook Jeong^{a,b,**}, John I. Risinger^{a,b,*}^a Department of Obstetrics, Gynecology and Reproductive Biology, Michigan State University, Grand Rapids MI, USA^b Spectrum Health, Grand Rapids MI, USA^c Department of Pathology, University of Texas MD Anderson Cancer Center, Houston TX, USA^d Department of Gynecological Oncology & Reproductive Medicine, University of Texas MD Anderson Cancer Center, Houston TX, USA^e GenEpria Consulting Inc., Columbia MD, USA

ARTICLE INFO

Keywords:

Cancer research
Immunology
Genetics
Women's health
Reproductive system
Oncology
Alternative medicine
Laboratory medicine
Clinical research
Endometrial cancer
Metastasis
Orthotopic tumor model

ABSTRACT

Endometrial cancer is the most common gynecologic malignancy in the U.S. with metastatic disease remaining the major cause of patient death. Therapeutic strategies have remained essentially unchanged for decades. A significant barrier to progression in treatment modalities stems from a lack of clinically applicable *in vivo* models to accurately mimic endometrial cancer; specifically, ones that form distant metastases and maintain an intact immune system. To address this problem, we have established the first immune competent murine orthotopic tumor model for metastatic endometrial cancer by creating a green fluorescent protein labeled cell line from an endometrial cancer that developed in a *Pgr^{cre/+}Pten^{f/f}Kras^{G12D}* genetically engineered mouse. These cancer cells were grafted into the abraded uterine lumen of ovariectomized recipient mice treated with estrogen and subsequently developed local and metastatic endometrial tumors. We noted primary tumor formation in 59% mixed background and 86% of C57BL/6 animals at 4 weeks and distant lung metastases in 78% of mice after 2 months. This immunocompetent orthotopic tumor model closely resembles some human metastatic endometrial cancer, modeling both local metastasis and hematogenous spread to lung and has significant potential to advance the study of endometrial cancer and its metastasis.

1. Introduction

An estimated 61,880 new patients will be diagnosed with endometrial cancer in 2019 making it the most common gynecologic malignancy in the United States and the fourth most common cancer in women [1]. Metastatic disease represents the major cause of death with five-year survival predicted to be 16.2% if distant spread is present [2, 3, 4, 5]. Although survival is so poor for patients with metastases the treatment modalities have remained essentially unchanged for several decades [6, 7] and unlike many other types of cancer the prevalence of endometrial cancer is increasing overall [2, 3, 8]. Currently, surgical staging is used to define the extent of disease as well as the risk of recurrence. In combination with surgical staging, pathologic classification is used to dictate the course of treatment for these women [9, 10, 11, 12, 13, 14, 15].

Recently, molecular features such as DNA mutation frequency and copy number changes have been proposed to more accurately predict future tumor behavior by dividing this cancer into four subgroups [16]. These groups are 1) copy number low, typically low-grade endometrioid histotypes that are microsatellite stable (MSS), with near diploid genomes and frequent *PTEN*, *KRAS*, *ARID1A*, *CTNNB1* and *AKT* mutations, 2) copy number high (CNH) high-grade cancers with frequent genomic gain and loss typified by serous histology and *TP53* mutation, 3) the hyper-mutated microsatellite instability-high (MSI-H) group of endometrioid type histology with a defect in DNA mismatch repair and 4) an ultra-mutated group characterized by high-grade endometrioid cancers with defects in the polymerase epsilon (*POLE*) gene exonuclease domain (ultra-mutant **POLE**). These four molecular classifications, in particular the **POLE** and **MSI-H**

* Corresponding author.

** Corresponding author.

E-mail addresses: jeongj@msu.edu (J.-W. Jeong), risinge4@msu.edu (J.I. Risinger).¹ Equal contribution.

groups, highlight a significant role for the patient's immune system in controlling spread of their endometrial cancer and define distinctive prognostic markers [17, 18, 19, 20, 21, 22, 23]. For example, the ultra-mutant POLE group consists of high-grade cancers which is a pathological feature associated with poor patient outcome. Despite being high-grade, cancers in this group rarely metastasize to cause patient death [16]. The favorable outcomes experienced by these patients are thought to be due to active immune recruitment and surveillance of tumor cells. Supporting studies have shown that these tumors have increased tumor infiltrating lymphocytes (TIL) and upregulated expression of TIL markers [17, 18]. Furthermore, recent evidence suggests that some endometrial cancers may respond particularly well to immune therapies and the MSI group is specifically targeted for response to these therapies [20]. An understanding of why these particular cancers have a favorable response to immune-based therapies could lead to novel therapeutic strategies for other endometrial cancers. These studies highlight the necessity of an intact immune system in clinically relevant animal models for endometrial cancer.

The lack of clinically appropriate animal models, in part, constrains the development of novel therapeutic strategies for endometrial cancer [24]. For example, classical subcutaneous models in nude mice fail to accurately represent the true progression of this disease due to lack of an immune system and incorrect microenvironment [24, 25, 26, 27, 28]. Genetically engineered animals are an improvement over models that utilize immunodeficient animals in that they maintain an immune system and develop disease in the uterus however, many of these mouse strains have a long latency period and do not develop metastatic disease at relevant sites [29, 30, 31, 32, 33]. In addition to these the BDI/Han rat strain spontaneously develops hormone dependent endometrial cancer [34]. While the rat model offer options for studying hormonal aspects of endometrial cancer, the cancers that develop in the rats lack the *Pten* mutations typical of hormone dependent endometrioid tumors in women [35]. Despite some of these drawbacks several uterine specific models reliably develop endometrial cancer [29, 30, 36, 37]. Of these models, all but one developed by Li, et al [37], either fail to develop metastasis or do not lend to extensive study of metastatic disease due to aggressive primary tumor formation and early death of the animal prior to distant metastasis and none are easily amenable to specific genetic manipulation within tumor cells (e.g. CRISPR/Cas-9 or gene overexpression).

The *PTEN* gene is one of the most commonly mutated genes across human cancers and functions as a tumor suppressor [38, 39]. *PTEN* is mutated in >50% of endometrioid endometrial cancers and about 20% [40] of endometrial hyperplasia, a precancerous endometrial lesion, highlighting its central importance in endometrial tumorigenesis [41]. In addition, up to 35% of endometrial cancers have activating oncogenic codon 12/13 mutations in the guanine nucleotide binding protein *KRAS* [42]. This mutation has also been reported in complex atypical hyperplasia of the endometrium suggesting that as with *PTEN* that it also plays an early role in the progression to endometrial cancer [43]. These two mutations occur predominately in endometrioid type cancers. Our model is therefore best classified as a model of type I endometrial cancer, endometrioid type with driver mutations consistent with the copy number low MSS molecular classification group. Given their prevalence, propensity of co-occurrence, and pathologic roles we chose to develop a mouse model of endometrioid endometrial cancer centered around defects in these genes.

In this manuscript, we describe an orthotopic transplant mouse model of endometrial cancer driven by *PTEN* deletion (*Pten*^{-/-}) and K-Ras activation (*K-Ras*^{G12D}) that originates in the uterus with an intact immune system and correct microenvironment. Tumor growth over time results in local extension and with hematogenous metastases at later time points. The growth characteristics of this model allow for the exciting opportunity to study disease progression over time from primary tumor formation to distant metastasis.

2. Results

2.1. Generation and characterization of MECPK cells

To begin development of an immunocompetent orthotopic model we first created an immortal cell line from an endometrial cancer that developed in a 4 week old *Pgr*^{cre/+}*Pten*^{f/f}*K-ras*^{G12D} genetically engineered mouse [30]. The resultant cell line was named MECPK (Mouse Endometrial Cancer *PTEN* deleted *K-ras* activated) and genotyping confirmed the expected *Pten* and *K-ras* genetic alterations. MECPK cells were transfected with a construct for green fluorescent protein (pSIH-H1-copGFP), and stable GFP expressing cells isolated. We purposely chose to label our cells with a construct lacking a selectable marker to allow for anticipated future experiments in which other genetic alterations necessitating antibiotic selection might be needed (e.g. CRISPR/Cas-9).

We further characterized these cells by western blotting. *PTEN* was absent in MECPK as compared to normal mouse uteri and consistent with the *PTEN* downregulation in endometrial tumors obtained from female *Pgr*^{cre/+}*Pten*^{f/f}*K-ras*^{G12D} animals (Figure 1 i). To examine whether *PTEN* loss resulted in expected downstream effects we assessed levels of phosphorylated AKT (Ser473) a known downstream effector of activated PI3K signaling. Phospho-AKT was elevated in MECPK with activations similar to *Pgr*^{cre/+}*Pten*^{f/f}*K-ras*^{G12D} animals and elevated as compared to non-malignant uterus (Figure 1 ii) while total AKT remained unchanged between each sample condition (Figure 1 iii). MECPK cells do not express estrogen (ESR1) or progesterone (PGR) receptors (Figure 1 iv-v).

We next tested whether MECPK cells still retain *in vivo* tumor forming ability. Tumors developed in 3 of 3 animals following subcutaneous injection in athymic nude (CrI:NU(NCr)-Foxn1^{nu}) mice at 2 weeks confirming that the cell line maintained the ability to form tumors.

2.2. Generation of orthotopic MECPK tumors

To develop better endometrial cancer models, we considered several factors. First tumors need to originate from the uterus and not be placed subcutaneous, intraperitoneal (I.P.) or in the renal capsule as with previous models [26, 28, 44, 45, 46, 47, 48, 49, 50, 51]. Further they need to develop in an immune competent background. We theorized that the previous failures of some to establish high rates of human patient-derived xenograft (PDX) engraftment in uterine horns might be for several reasons. Firstly, that the uterus itself might not be in a proliferative state and that this might inhibit engraftment. Additionally, unlike subcutaneous, renal capsule, or I.P. sites, a glycoprotein-rich, mucous-rich layer protects the uterine lumen. We hypothesized that this mucous layer may inhibit initial attachment of tumor cells to the epithelial layer. Therefore, we developed and tested the effect of two procedures to improve orthotopic grafting [1]: the effect of an abrasion in the uterine lumen [2], the role of a proliferative endometrium on tumor formation in an intact immune system.

2.3. Enhancement of successful *in utero* graft establishment through estrogen supplementation and mucosal abrasion

We utilized mixed background immune competent animals to evaluate the effect of estrogen supplementation and uterine luminal abrasion on tumor formation. Briefly, three days prior to the start of the experiment, immune competent female mice were injected with exogenous estrogen once daily for three days (0.1 µg/injection). On the date of cell injection (considered day 0) animals were ovariectomized (OVX), the uterine lumen was either abraded using a blunted 25G needle (abrasion) or not abraded (no abrasion) and 500,000 MECPK-GFP cells were injected. We examined uteri and tumor formation in estrogen stimulated (E2) and control (vehicle) mice after 4 weeks (n = 5, 8, and 17 for vehicle + abrasion, E2 + no abrasion, and E2 + abrasion respectively, Table 1). Mice lacking exogenous estrogen supplementation (vehicle + abrasion) failed to develop tumors (0%) while the majority (59%) of luminal abraded mice

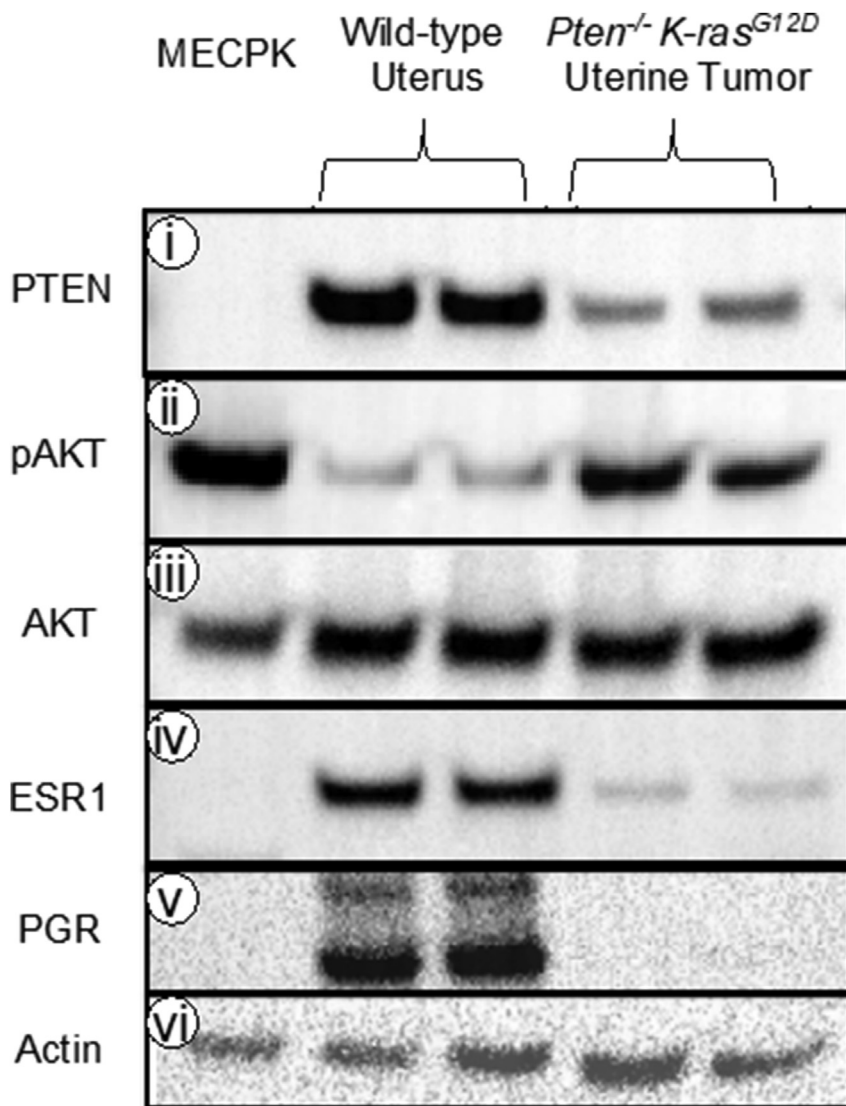


Figure 1. Protein expression profile of MECPK cells, normal uterine tissue, and *Pten*^{-/-} *K-ras*^{G12D} uterine tumor. Western blot analysis of PTEN, Phospho-AKT (pAKT), AKT, PGR, and ESR1 in MECPK cell line extract as compared to normal uterine tissue and uterine tumor tissue from *Pten*^{-/-} *K-ras*^{G12D} mice. i) MECPK cells completely lack PTEN as compared to normal uterine tissue and tumor tissue samples indicating purity of the cell line and lack of stromal contamination as seen in the faint banding of the tumor samples. ii) MECPK and mouse uterine cancers have elevated levels of pAKT as compared to normal uterine tissue while total AKT (iii) between the samples remained relatively constant. iv-v) Both estrogen and progesterone receptors (ESR1 and PGR) are undetectable in the MECPK cell line. vi) β -actin serves as the loading control. 10 μ g protein/lane. Membranes were stripped and re-probed for each antibody. Full, non-adjusted images of blots are provided as Supplemental Figure 4.

with estrogen stimulation (E2 + abrasion) developed uterine tumors ($p = 0.0396$). In contrast, mice treated with estrogen but lacking abrasion (E2 + no abrasion) rarely developed tumors. Those abraded uteri were more likely to develop tumors as opposed to non-abraded ($p = 0.04$). Thus, we concluded that mucosal abrasion enhanced graft establishment and likely provides an adherent surface for the injected cells. All subsequent experiments were conducted with the use of exogenous estrogen

supplementation and mucosal abrasion (Figure 2A). Grossly evident primary tumors developed in 10 of 17 (59%) mice after 1 month in these mixed background mice (Figure 2B i and Table 1). Further we utilized a fluorescent dissection microscope to distinguish GFP positive tumor cells (Figure 2B ii). The invasive nature of the cells was also observed by GFP label in frozen sections and GFP labeled cancer cells infiltrated the deeper uterine tissue layers (Figure 2B iii-iv).

Table 1. Summary of one month gross tumor formation in mixed background or C57BL/6 mice. * $p = 0.04$ indicating significantly increased take-rate with estrogen supplementation vs. non-estrogen supplemented; * $p = 0.04$ indicating increased take-rate between estrogen supplemented groups with or without abrasion; # $p = 0.13$ indicating no significant differences between mixed background and C57BL/6 tumor establishment rates.

Mixed Background 1 Month	Tumor	No Tumor	Total Animals Observed	Tumor Development (%)
Vehicle + Abrasion	0	5	5	0% *
E2 + No Abrasion	1	7	8	13% †
E2 + Abrasion	10	7	17	59% *†#
C57BL/6J Background 1 Month	Cancer	No Cancer	Total Animals Observed	Cancer Development (%)
E2 + No Abrasion	0	3	3	0%
E2 + Abrasion	12	2	14	86% #

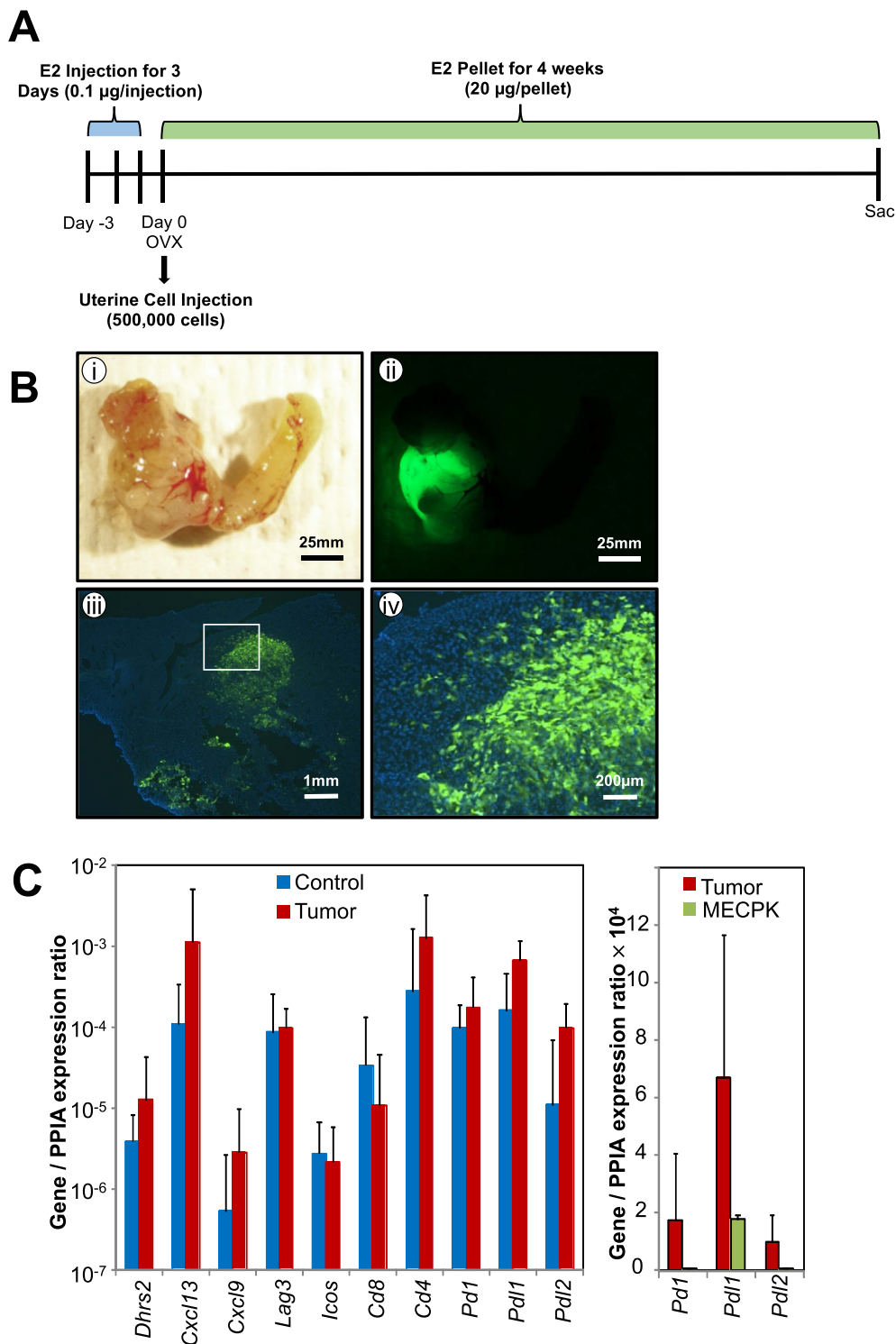


Figure 2. MECPK model method, primary tumor formation, and immune gene expression. A) Summary of graft protocol. For three consecutive days prior to surgery, mice were injected with 0.1 µg of estrogen. The distal ends of the uterine horns were ligated and the ovaries removed (OVX) on the day of surgery. 500,000 cells were injected into one horn suspended in a 1:1 mixture of PBS:Matrigel. The second horn was left as a control and received a sham surgery. B) Representative tumor formation in a mixed background immune-competent mouse (i) with corresponding detection of GFP labeled cells (ii). GFP labeled cancer cells invade into uterine wall (iii-iv). C) Immune gene expression in normal uterine (control) $n = 3$ and tumor bearing uterine tissue (tumor) $n = 3$ (left). Selected immune gene expression in MECPK-GFP cells (right). Immune gene expression was normalized to *Ppia*, a housekeeping gene.

2.4. Characterization of primary and metastatic MECPK tumors

The MECPK model demonstrates tumor growth in the context of an intact immune system. With this in mind, we chose to examine the expression of several key immune signature genes representing B and T-cell chemo attractants (*Cxcl13*, *Cxcl9*), MHC Class II ligands (*Lag3*, *Cd4*), markers of activated T-cells (*Icos*), and MHC class I markers (*Cd8*) that are known to infiltrate human endometrial cancers and which may be drastically elevated in some MSI and many POLE immune-infiltrated and activated cancers [21, 22, 23]. RNA

expression of *Dhrs2*, *Cxcl13*, *Cxcl9*, *Lag3*, *Icos*, *Cd8*, and *Cd4* did not differ significantly between the grafted uterine horn with tumor and the control uterine horn at one-month post cell injection (Figure 2C left. $n = 3$ independent animal samples per group). These data show that mRNA levels of the key modulators of immune surveillance, *Pd1*, *Pdl1*, and *Pdl2*, were not highly expressed in the MECPK-GFP cell line (Figure 2C right). Based on these results we concluded that our graft procedure as well as the MECPK-GFP cells themselves do not inherently induce an immune response or express immune markers.

We performed a molecular and histological characterization of MECPK uterine tumors (n = 3, Figure 3A). Histological analysis and Ki67 immunoreactivity confirmed these lesions were highly proliferative high-grade endometrial cancers (Figure 3A i-vi). As expected, PTEN was not detected in tumor cells (Figure 3A vii-ix). PI3K and MAPK pathway activation in tumors were evaluated using phospho-specific antibodies. Tumor cells expressed phospho-AKT (Ser473) and pERK1/2 (Thr202/Tyr204) (Figure 3A x-xxi). Primary tumor cells were Vimentin variable diffuse positive and CDH1 (E-Cadherin) positive (Figure 3A xii-xxvii).

Tumor histology from our *in vivo* model was evaluated by H&E staining (Figure 3B i). We found that *in vivo* tumor formation displays histological characteristics similar to that of high-grade human disease (Figure 3B ii-iii). Notably, cells were tightly compacted, with absent glandular features, numerous visible mitotic events and near complete loss of stroma.

Metastasis is a complex process and local extension metastasis to ovaries adnexa etc of this model likely proceeds by different mechanisms than does the establishment of metastasis in the lung and liver. Above data suggest that MECPK tumor cells express both Cdh1 and Vim. Our MECPK model expresses Cdh1 and Vim mRNAs as well as their transcriptional regulators snail and slug when cultured *in vitro* (data not shown). We performed an additional analysis of the expression of these classical markers of epithelial mesenchymal transition in the paired primary uterine lesion and metastatic lung lesions (Supplemental Figure 1). We confirmed the expected staining in normal uterine tissues which show strong Cdh1 staining in the epithelial cells of the lumen and glands of the uterus and absent expression in stroma. Vimentin, however is expressed in the stroma and largely absent in normal endometrial epithelia. Cdh1 and Vim staining patterns were similar in lesions from the primary uterine tumor and from the lung lesions with tumor cells retaining expression of Cdh1 and also exhibiting moderate Vim staining in some but not all cancer cells (Supplemental Figure 2).

Given the expression characteristics of the tumor cells and in particular the variable vimentin expression we sought to characterize the tumor heterogeneity. Cancer stem cells are proposed for endometrial cancer but no consensus marker has been confirmed to assess them. Cd133 (Prominin-1) an endothelial expressed gene that is considered enriched in cancer stem cells of several different malignancies including endometrial cancer is one proposed endometrial cancer stem cell marker [52, 53]. We performed quantitative PCR on lesions isolated from primary tumors and metastatic lung lesions and noted moderate Cd133 expression (Supplemental Figure 3A). Given that Cd133 was expressed in at least some tumor cells we further investigated primary uterine and metastatic lung lesions by IHC to determine whether Cd133 was enriched in any specific tumor regions or metastasis. We noted strong staining of Cd133 in perivascular areas of blood vessels as expected and heterogenic staining in tumor cells without obvious enrichment in metastatic lesions (Supplemental Figure 3B).

2.5. MECPK animals die of metastatic cancer

We evaluated the effect of long-term tumor growth of the MECPK model and determined the natural course of disease progression. We initiated MECPK tumors in eleven mixed background, uterine abraded, immune competent animals supplemented with exogenous estrogen and evaluated end of life as determined by either humane endpoint or unexpected death from disease days post injection (DPI). In this experiment, animals expired as early as 35 days and survived as long as 125 DPI (Figure 4A n = 11, two censorships due to unexpected death. Median survival was 76 DPI). Necropsy of expired animals confirmed bulky uterine disease in the 9 animals that were recovered. In addition, extensive cancer growth was evident in lungs of almost all the animals which was likely the cause of their death (Figure 4B ii).

2.6. Metastatic spread in the MECPK model

Our survival experiment indicated frequent metastases in the lungs of MECPK implanted mice. Therefore, we carefully characterized the rates of the metastatic spread of MECPK cells both at long and short-terms. Nine of the 11 animals (two censorships due to unexpected death) from above experiment were included in the long-term group analysis. The short-term animal group included a sub-cohort of 8 out of 17 animals from the mixed background one month study which show the presence of primary tumor. From these 8 animals evaluated, all also had local extension spread outside of the uterus (Table 2). Additionally, in 1 of 8 animals we were able to detect distant spread of disease in the lung (Figure 4B iii-iv). At two months, in addition to primary tumor and local extension of disease (Figure 4B i) in all 9 animals evaluated, we found distant disease in the lung (Figure 4B ii) in 7 of them (Table 2). To further characterize the distant disease, H&E sections were made from the lungs of animals at one month and two months post injection (Figure 4C i-iv). At one month, small nests of micro metastatic disease were present (Figure 4C i, iii, n = 3) while at two month and later, larger and solid tumor areas had formed (Figure 4C ii, iv). Other rare sites of metastatic disease were present, specifically liver, spleen and cutaneous lesions at a frequency of 8%, 4% and 4% respectively (Table 3).

2.7. Tumor formation in C57BL/6 mice

To test whether MECPK-GFP cells could grow in the commonly available C57BL/6 background, we implanted OVX female C57BL/6 mice supplemented with exogenous estrogen with (n = 14) or without luminal abrasion (n = 3) (Table 1). C57BL/6 mice provided with exogenous estrogen but lacking abrasion failed to develop tumors (n = 3). C57BL/6 mice supplemented with exogenous estrogen and abrasion developed cancer in 12 out of 14 animals (n = 14; 12 with cancer, 2 without cancer, p = 0.015). Cancer development in the uterus of the C57BL/6 strain was not statistically significantly different than development in the mixed background strain (p = 0.13).

3. Discussion

Here we describe the development and characterization of the first immunocompetent orthotopic murine model of endometrial cancer. Our model is based on the implantation of the MECPK cell line, which is derived from primary endometrial tumors of *Pgr^{cre/+}Pten^{f/f}K-ras^{G12D}* mice [30]. MECPK tumors very closely mimic high-grade human endometrioid type endometrial cancers. Tumors exhibit loss of PTEN, activation of K-Ras, PI3K and MAPK pathway activation, and elevated Ki67 immunoreactivity, thereby confirming these lesions were highly proliferative. Because tumors in MECPK implanted mice possess the well-known genetic defects and established drivers of human endometrioid endometrial cancer and exhibit the expected activation of AKT and ERK pathways, we anticipate this model will be useful for the evaluation of targeted therapeutics aimed at modulating these specific pathways.

Primary tumor cells were displayed variable diffuse positivity of Vimentin and were CDH1 positive. This model develops frequent distant lung metastasis allowing for the preclinical evaluation and treatment of disease spread from early micro-metastatic stages onward. Importantly MECPK tumors grow with equal frequency and exhibit the same tumor proclivity characteristics in the commercially available and fully immunocompetent C57BL/6 mice.

Endometrial cancers from MECPK implanted mice result from defects in well-known and established drivers of human endometrioid endometrial cancer and exhibit the expected activation of AKT and ERK pathways. As such this model should be useful for drug studies examining targets aimed at modulating these specific pathways. Our model circumvents many deficits of other current models of endometrial cancer, specifically, those models that either do not metastasize or developed in immune deficient mice, which limit the scope of biological processes that

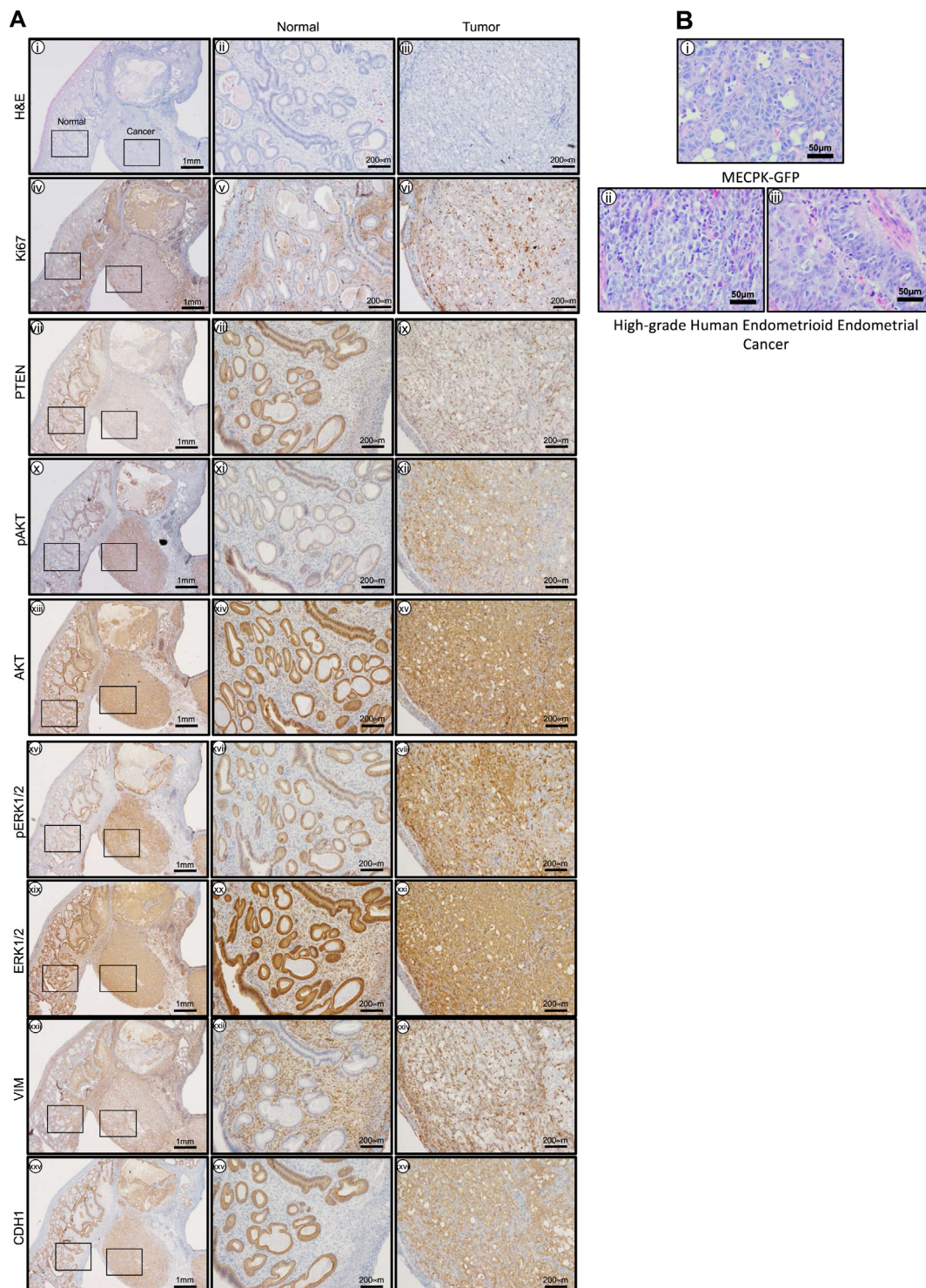


Figure 3. Histological characteristics of endometrial tumors formed in the *Pten*^{-/-} *Kras*^{G12D} MECPK model. A) i) Low magnification (4X) (left) showing tumor tumor interface with normal tissue and high magnification (20X) of ii) normal (center) and iii) cancer tissues (right) with H&E. H&E of tumors from *Pten*^{-/-} *Kras*^{G12D} MECPK mice are endometrioid, lack glandular formation, and have minimal stroma. Ki67 confirmed these lesions were highly proliferative. iv-vi). As expected, PTEN was not detected in the cancer cells of the tumor tissue (vii-ix). Tumors expressed pAKT (x-xii), AKT (xiii-xv), pERK1/2 (xvi-xviii) and ERK1/2 (xix-xxi) important markers of PI3K and MAPK activation. Primary tumors were Vimentin positive in stroma and largely negative in epithelium and cancer cells (xxii-xxiv) and were negative for CDH1 in the stroma and positive in normal epithelium and in cancer cells (xxv-xxvii). n = 3 independent tissue samples. B) Comparison of MECPK tumor histology to human endometrial cancer samples. i) Representative H&E of a MECPK tumor at 1 month post-injection. *In vivo* tumor formation displays histological characteristics similar to that of grade 3 endometrioid endometrial cancers (ii-iii). Notably, cells are tightly compacted with visible mitotic events and near complete loss of stroma. Scale bar: 50 μm.

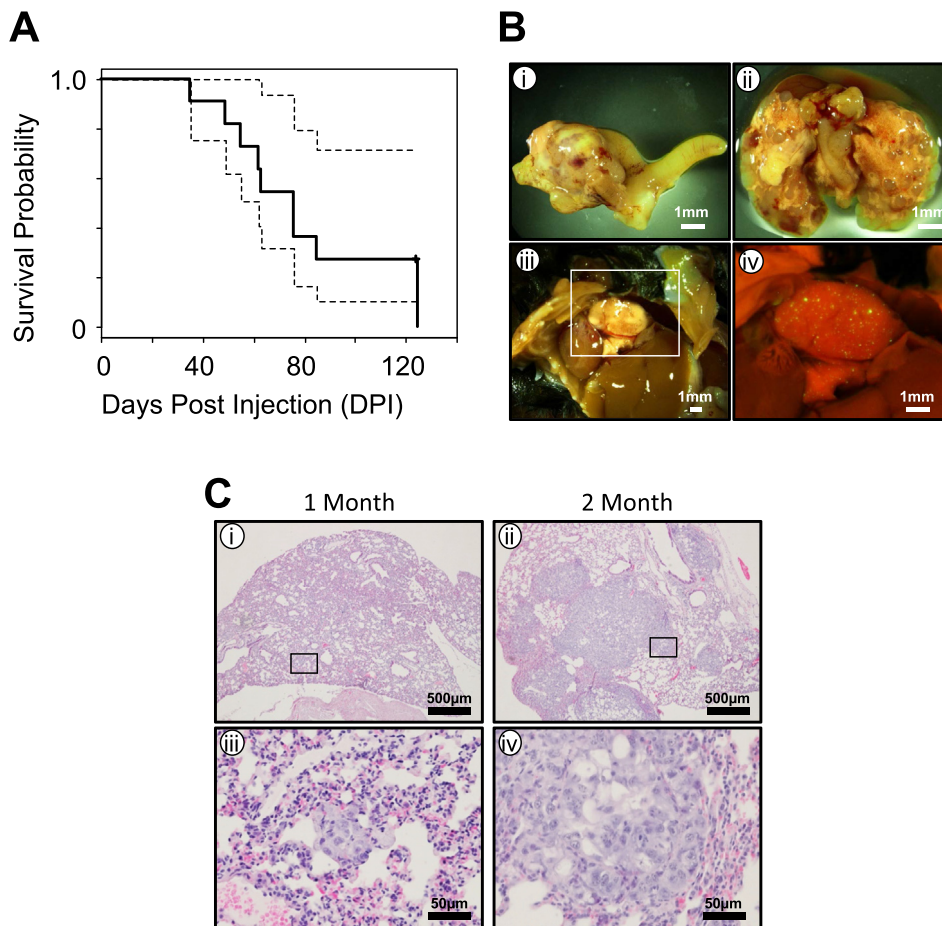


Figure 4. Survival and characterization of metastatic spread for *Pten*^{-/-}*Kras*^{G12D} MECPK model. A) Survival plot showing natural course of disease. N = 11 including two censored cases. Median survival = 76 DPI. Dashed lines are 95% confidence limits. B) Representative image of primary uterine tumor and metastatic lung spread at 6 weeks post cell injection (i-ii). GFP detection of non-macroscopic metastatic spread to the lung at four weeks post-injection (iii-iv). C) H&E sections showing progression of lung disease at 1 and 2 months post-uterine injection. At one month (i), micro-metastatic is detectable through histologic analysis (iii). At two months (ii), larger tumor cell nests are present in the lungs (iv).

Table 2. Summary of metastatic lung disease development over time. Notably, the rate of distant metastatic disease detected in the lung drastically increases if allowed to grow past one month. Experiments were conducted as described in Figure 2A. Constant estrogen stimulation was maintained through subcutaneous placement of a 20 µg estrogen beeswax pellet. Pellet was replaced every 4 weeks until a death or a humane endpoint was reached as determined by primary tumor volume or obvious signs of animal distress.

Time Point	Local Metastasis	Distant Metastasis	Total Animals Observed	Chance of Distant Metastasis
Short-Term (1 Month)	8	1	8	13%
Long-Term (Over 1 Month)	9	7	9	78%

can be studied. Further, classical subcutaneous models in nude mice lack an immune system response and maintain tumors in an incorrect microenvironment, which could impact study outcomes. While genetically engineered animals are an improvement over classic nude animal models, many still have a long latency period and/or do not develop metastatic disease.

Our model resembles high-grade human endometrial cancer histologically as it lacks appreciable stroma and progresses as high-grade human endometrial cancer would *in vivo* specifically metastasizing to the most common site of hematogenous spread - the lung [54, 55]. Interestingly MECPK cells lack ESR1 and PGR, which is associated with

Table 3. Summary of observed metastatic site rates. N = 26 animals observed across all time points. Only animals which had confirmed primary tumor formation were considered when calculating percentages.

Metastatic Site	%Observed
Lung	31%
Liver	8%
Spleen	4%
Cutaneous	4%

high-grade disease in humans [56, 57, 58, 59]. Normal endometrial tissue is both estrogen and progesterone sensitive. We noted enhanced graft take-rates upon exogenous estrogen supplementation despite the lack of detectable protein levels of estrogen receptor in MECPK cell lysate (Figure 1 iv). While supplemented estrogen may not be working directly on the injected cells from the cell line, it is likely stimulating stromal tissue as has been shown previously [60] in the normal uterus prior to cell injection increasing its size and potentially enhancing the microenvironment to favor the proliferative tumor cells. Estrogen impacts epithelial permeability through modulation of tight junction proteins in the endometrium and cervix [61, 62, 63] leading to increased barrier permeability and allowing injected tumor cells to more easily invade past the epithelium and into deeper tissue layers of the uterus. Additionally, estrogen is a known modulator of vascular growth in the uterus [64] and may be contributing to increased vascularization and favorable growth conditions for resultant tumors as well as an increased potential for hematogenous spread to the lungs. With ovariectomy in our methodology we have eliminated the possibility of ovarian produced progesterin, the normal signal for tissue growth to cease thus favoring continuous growth. Together these factors may potentially provide optimal conditions for unopposed tumor growth in this model and improving overall tumor establishment rates.

One of the most important aspects of this model is that MECPK endometrial tumors and their metastases develop in the presence of an intact immune system. We performed an initial characterization of several immune cell markers previously shown to be upregulated in human endometrial cancers with increased immune infiltrate. We did not note any transcriptional change in key immune markers *Dhrs2*, *Cxcl13*, *Cxcl9*, *Lag3*, *Icos*, *Cd8*, and *Cd4*. MECPK model tumors would be most similar to the copy number low MSS molecular classification group based on the lack of a prominent T-cell infiltrate which is present in endometrioid cancers with MSI and POLE mutation. Consistent with these findings is that MECPK cells express mismatch repair proteins and lack mutation in the exonuclease domain of Polymerase-E (data not shown). We did note that *Pd1*, *Pdl1*, and *Pdl2* were not elevated in our cell line. Levels of *Pd1* are important because the interaction between PD-1 with PD-L1 has been demonstrated to inhibit antigen sensitization in peripheral T cells in this way, protecting normal tissues against self-injury from the immune system. PD-L1 has been shown to be expressed in 11–83% of primary endometrial cancers and in 96% of metastatic samples and thus may serve as an immune target [65, 66]. Future studies will address expression of these genes *in vivo*.

Utility of true syngeneic models are limited by the availability of the background strain. Importantly we demonstrated that MECPK cells grow equally as well in C57BL/6 mice using the same protocol as was used in the mixed background animals. Our results indicated similar success rates between the strains. Indeed, this should not be surprising as the cell line originated from mixed C57BL/6J x 129 background. It is known that each particular laboratory mouse strain is homozygous and has its own unique major histocompatibility haplotype. C57BL/6J and 129 backgrounds harbor the same haplotype and thus graft rejection should not be an issue when switching from the mixed to C57BL/6J background [67]. With this in mind, our model should make an impact like other similar models such as the ID8 model for ovarian cancer and the RUC1A1 rat endometrial cancer model [68, 69]. However, unlike ID8 which spontaneously transformed and lacks known drivers of ovarian cancer, our model is driven by PTEN deletion and K-Ras activation: established and well-known drivers that are present and highly prevalent in human endometrial cancers.

We have demonstrated the exciting potential for further utility of our model by adding a GFP label to the MECPK cell line suggesting that *in vitro* manipulation of the cell line can be conducted prior to injecting cells. These cells can then be subject to other manipulations either adding additional oncogenic or deleting specific tumor suppressor or DNA repair gene capabilities which are established factors in defining the newly described molecular sub-groups and perhaps impacting their growth rate or metastatic potential.

4. Conclusions

Here we have described the first orthotopic mouse model of endometrial cancer in a fully immunocompetent animal. Our model has several significant advantages over current xenograft models. Injection of cancer cells orthotopically allows for tumor cell exposure to the physiologically appropriate microenvironment. Further, the presence of an intact immune system allows for the exciting potential to study immunotherapies and immune interactions with cancer cells. Finally, specific genetic modifications dictated by the investigator can be made to the cell line *in vitro* prior to grafting, and thus can alter the future *in vivo* tumor for study. These features allow for ease of study of both *in vivo* tumor formation and *in vitro* cell line manipulation.

5. Materials and methods

5.1. Guidelines for animal research

Mice were maintained in the designated animal care facility at the Van Andel Institute according to Michigan State University's institutional guidelines for the care and use of laboratory animals. Experimental protocols were reviewed and approved by the Michigan State University

Institutional Animal Care and Use Committee (IACUC) and the Van Andel Institute.

5.2. Mouse strains

Mixed background: C57BL/6 × 129 females ages 8 weeks or greater received an injection of 500,000 cells into one uterine horn with or without abrasion technique. Sacrifice and evaluation for tumor formation was performed at various time points as described.

C57BL/6: 8-week-old female animals (The Jackson Laboratories. Bar Harbor, ME USA) were injected with 500,000 cells into one uterine horn after abrasion technique was performed. Sacrifice and evaluation for tumor formation was performed 1 month after injection.

Athymic nude (CrI:NU(NCr)-Foxn1^{nu}): Animals were injected (n = 3) with 500,000 cells into one uterine horn after abrasion technique was performed. After 2 weeks of growth, animals were sacrificed and evaluated for tumor formation.

5.3. MECPK cell line establishment

A small piece of uterine tumor from a 4-week-old female *Pgk^{Cre/+} Pter^{f/f}K-Ras^{G12D}* animal was finely minced, placed into a 10-cm plate, and maintained in DMEM supplemented with 10% fetal calf serum, and in the presence of antibiotic/antimycotic (Gibco, Thermo Fisher Scientific, Waltham, MA USA). Tumor cells were established and fibroblasts were removed over time by gentle scraping. Pure tumor cultures were passaged more than 70 times. The resultant endometrial cancer cell line, Mouse Endometrial Cancer Pten deleted Kras activated (MECPK) was maintained and grown in Dulbecco's Modified Eagle's Medium with F12 (Invitrogen, Thermo Fisher Scientific, Waltham, MA USA), supplemented with 10% (v/v) fetal bovine serum (Invitrogen), 50 units/ml penicillin and 50 µg/ml streptomycin (Invitrogen) in an atmosphere of 5% CO₂ and 95% air at 37 °C. The MECPK-GFP line was generated by transfecting unlabeled MECPK cells with pSIH-H1-copGFP (SI501A-1, System Biosciences Inc.). Since no selection marker is present on this plasmid, single-cell seeding was subsequently performed to obtain a GFP-labeled clone.

5.4. Endometrial priming for receipt of tumor cells and in utero cancer cell injection

Female mice (average age 12.5 weeks) were injected with 100 ng of E2 per day for three days prior to cell engraftment. On the day of cellular injection (considered experimental Day 0), a small incision was made on the left flank of the animal anterior to the femur and lateral to the spine. The ovary was visualized through the inner pelvic fascia and a deeper cut into the pelvic cavity was made to expose the ovary. Forceps were used to pull the left uterine horn and ovary outside of the body cavity. A blunted 25G needle was inserted into the uterine lumen and used to mechanically abrade the luminal mucus layer along the full length of the anti-mesometrial 500,000 MECPK-GFP cells were suspended in 50 µl of a 1:1 mixture of Matrigel (Corning, Corning, NY USA) and PBS and injected into the abraded uterine lumen using a 25G needle. We confirmed that our abrasion technique was not directly seeding the injected cancer cells into the blood by comparing abraded animals to tail vein injected animals and looking for GFP labeled cancer cells in the lungs (Supplemental Figure 1). Animals were bilaterally ovariectomized (OVX) at the time of cell injection and a 20 µg estrogen beeswax pellet (replaced every 4 weeks) was placed under the skin at the base of the posterior neck between the shoulder blades. The right uterine horn was left intact as a sham control after OVX. The mice were sacrificed at 1 month for short-term experiments and at a humane endpoint in long-term disease course experiments (as determined by palpable primary tumor volume, external signs of animal distress, or death). Following death, mouse uteri were then excised, weighed and fixed in 4% paraformaldehyde for histological analysis.

5.5. Western blot analysis

Tissue and cell line samples containing 15 µg of protein were applied to SDS-PAGE 8–12% Bis-tris gel. The separated proteins were transferred onto a polyvinylidene difluoride membrane (Millipore Corp. Burlington, MA USA). Membranes were blocked overnight with 0.5% casein (wt/vol) in Phosphate Buffered Saline with 0.1% Tween 20 (vol/vol) (PBS-T) (Sigma-Aldrich. St. Louis, MO USA) and probed with anti-PTEN (9188, Cell Signaling), pAKT (4060, Cell Signaling), AKT (4691, Cell Signaling), anti-PR (DAKO Corp. Carpinteria, CA USA), or anti-ER α (DAKO Corp.) antibodies. Immunoreactivity was visualized by incubation with a horseradish peroxidase-linked secondary antibody and treatment with ECL reagents (Advansta. Menlo Park, CA USA). Membranes were stripped and re-probed for each antibody using Re-blot Plus Mild Solution (2502, Millipore). To control for loading, the membrane was stripped and probed with anti-actin (Santa Cruz Biotechnology Inc. Santa Cruz, CA USA) and developed again.

5.6. Immunohistochemistry

Uterine sections from paraffin-embedded tissue were cut at 6 µm and mounted on silane-coated slides, deparaffinized, and rehydrated in a graded alcohol series. Sections were pre-incubated with 10% normal horse serum in PBS (pH 7.5) and then incubated with anti-Ki67 antibody (BD550609. BD Pharmingen) or anti-PTEN (9188, Cell Signaling), pAKT (4060, Cell Signaling), AKT (4691, Cell Signaling), ERK1/2 (4695, Cell Signaling), pERK1/2 (4370, Cell Signaling), Vimentin (ab92547, Abcam), E-cadherin (M-106, Takara), Cd133/Prominin (monoclonal 13A4, Invitrogen) in 10% normal serum in PBS (pH 7.5). On the following day, sections were washed in PBS and incubated with a secondary antibody (5 µl/ml; Vector Laboratories. Burlingame, CA USA) for 1 h at room temperature. Immunoreactivity was detected using the DAB kit (Vector Laboratories, Burlingame, CA USA).

5.7. Frozen sections

Tissue was fixed in 4% paraformaldehyde (PFA) (O4042-500, Fisher) in PBS for 6 h at 4 °C. Tissue was then washed in PBS for 5 min followed by cryoprotection in ice cold Hanks' Buffered Salt Solution (HBSS, 14170, Gibco) containing increasing concentrations of sucrose (10%, 15%, 20%, S-1888, Sigma) at 4 °C until evidence of osmotic equilibration as indicated by sinking tissue. Tissue was then embedded directly in base mold (22038218, Fisher) on top of dry ice with OCT (4853, Tissue-Tek) and allowed to solidify for several hours. 6 µm sections were obtained on a cryostat and tissue counterstained with DAPI to detect GFP (VECTA-SHIELD Mounting Medium with DAPI, H-1200, VECTOR).

5.8. Quantitative real-time PCR

Flash frozen samples were subject to total RNA isolation with TRIzol Reagent (Ambion. Thermo Fisher Scientific, Waltham, MA USA) according to manufacturer's recommendation. Then two µg of RNA were first treated with OPTIZYME DNase I (Thermo Fisher Scientific. Waltham, MA USA) for the preparation of DNA-free RNA prior to the transcription into complementary DNA (cDNA) with qScript cDNA Synthesis Kit (Quanta Biosciences. Beverly, MA USA). These cDNA were used as the template for the quantitative real-time PCR using primers with PerfeCTa SYBR Green FastMix reagent Quanta Biosciences (Beverly, MA USA) and the primers with the following sequences for *Dhrs2* forward 5'-ctgagaccgcccagcactctgtgac-3', reverse 5'-accagagggtgactccggccaca-3', *Cxcl13* forward 5'-gatcggatcaagttacgcccccctg-3', reverse 5'-ataactttctcatcttggtccaga-3', *Cxcl9* forward 5'-gctgtctttctcttgggcatca-3', reverse 5'-ggagcatcgtcactcttatact-3', *Lag3* forward 5'-agtgtacgcccagagctagctca-3', reverse 5'-acgagatggcctcttaaggtcac-3', *Icos* forward 5'-aggaaccttagtgaggatattgc-3', reverse 5'-ccctacgggtagccagagctcag-3', *Cd8* forward 5'-cggtgatgtactcagttctcgt-3', reverse 5'-ggatctcgcagcactgcttgta-3', *Cd4* forward 5'-

caggaagaggaggtgagttgtgg-3', reverse 5'-ttgcaacaggctgtaccggactg-3', *Pd1* forward 5'-acccaaggcaaaatcgaggag-3', reverse 5'-gctgggatatctgtgaggtct-3', *Pd11* forward 5'-atcagctacgttggtgctgacta-3', reverse 5'-ttctctggtgattttcggtat-3', and *Pd12* forward 5'-ccgctgggactacaagtactga-3', reverse 5'-acctccagatcctagtctatc-3', *Cd133* forward 5'-gcatctctctcaacgtg-3', reverse 5'-agttctgtctgtatgagtttt-3'. All qPCRs were done on Stratagene MX3000P and the mRNA quantities were normalized using mouse *Ppia* (cyclophilin A, 4333763F, Applied Biosystems) endogenous control.

5.9. Statistical analysis

The statistical significance of tumor formation e.g. by E2 in comparison with vehicle was assessed by setting up a 2 × 2 contingency table and calculation of two-tailed p-value by Fischer's exact test. The p-values were calculated separately for the comparisons: (i) Vehicle + abrasion vs. E2 + abrasion, (ii) E2 vs. E2 + abrasion, and (iii) mixed vs. C57BL/6 backgrounds. The significance of immune gene expression difference between tumor and control was assessed by two-tailed p-value of paired T-test. Calculations were done using Graphpad software (La Jolla, CA, USA) and survival package in R environment (<https://cran.r-project.org/>).

Declarations

Author contribution statement

Alyssa M. Fedorko: Performed the experiments; Analyzed and interpreted the data; Wrote the paper.

Tae Hoon Kim: Performed the experiments; Analyzed and interpreted the data.

Russell Broaddus, Rosemarie Schmandt, Gadisetti V.R. Chandramouli: Analyzed and interpreted the data; Contributed reagents, materials, analysis tools or data.

Hong Im Kim: Analyzed and interpreted the data.

Jae-Wook Jeong, John I. Risinger: Conceived and designed the experiments; Analyzed and interpreted the data.

Funding statement

This research did not receive any specific grant from funding agencies in the public, commercial, or not-for-profit sectors.

Competing interest statement

The authors declare no conflict of interest.

Additional information

Supplementary content related to this article has been published online at <https://doi.org/10.1016/j.heliyon.2020.e04075>

References

- [1] R.L. Siegel, K.D. Miller, A. Jemal, Cancer statistics, 2019, *Ca - Cancer J. Clin.* 69 (1) (2019) 7–34. Epub 2019/01/09 PubMed PMID: 30620402.
- [2] N. Howlader, A.M. Noone, M. Krapcho, J. Garshell, D. Miller, S.F. Altekruse, C.L. Kosary, M. Yu, J. Ruhl, Z. Tatalovich, A. Mariotto, D.R. Lewis, H.S. Chen, E.J. Feuer, K.A. Cronin (Eds.), SEER Cancer Statistics Review, 1975–2012, National Cancer Institute, Bethesda, MD, April 2015. https://seer.cancer.gov/archive/csr/1975_2012/.
- [3] R.L. Siegel, K.D. Miller, A. Jemal, Cancer statistics, 2016, *Ca - Cancer J. Clin.* 66 (1) (2016) 7–30. Epub 2016/01/09 PubMed PMID: 26742998.
- [4] P. Morice, A. Leary, C. Creutzberg, N. Abu-Rustum, E. Darai, *Endometrial cancer, Lancet* 387 (10023) (2016) 1094–1108. PubMed PMID: 26354523.
- [5] N.C. Institute, Cancer Stat Facts: Endometrial Cancer, 2017. Available from: <https://seer.cancer.gov/statfacts/html/corp.html>.
- [6] W.M. Burke, J. Orr, M. Leitao, E. Salom, P. Gehrig, A.B. Olawaiye, M. Brewer, D. Boruta, J. Villella, T. Herzog, F. Abu Shahin, *Endometrial cancer: a review and*

- current management strategies: part I, *Gynecol. Oncol.* 134 (2) (2014) 385–392. Epub 2014/06/07 PubMed PMID: 24905773.
- [7] W.M. Burke, J. Orr, M. Leitao, E. Salom, P. Gehrig, A.B. Olawaiye, M. Brewer, D. Boruta, T.J. Herzog, F.A. Shahin, Endometrial cancer: a review and current management strategies: part II, *Gynecol. Oncol.* 134 (2) (2014) 393–402. Epub 2014/06/15 PubMed PMID: 24929052.
- [8] R.L. Siegel, K.D. Miller, A. Jemal, Cancer statistics, 2015, *Ca - Cancer J. Clin.* 65 (1) (2015) 5–29. Epub 2015/01/07 PubMed PMID: 25559415.
- [9] H.M. Keys, J.A. Roberts, V.L. Brunetto, R.J. Zaino, N.M. Spirtos, J.D. Bloss, A. Pearlman, M.A. Maiman, J.G. Bell, A phase III trial of surgery with or without adjunctive external pelvic radiation therapy in intermediate risk endometrial adenocarcinoma: a Gynecologic Oncology Group study, *Gynecol. Oncol.* 92 (3) (2004) 744–751. Epub 2004/02/27 PubMed PMID: 14984936.
- [10] T.W. Kong, S.J. Chang, J. Paek, Y. Lee, M. Chun, H.S. Ryu, Risk group criteria for tailoring adjuvant treatment in patients with endometrial cancer: a validation study of the Gynecologic Oncology Group criteria, *J. Gynecol. Oncol.* 26 (1) (2015) 32–39. Epub 2014/11/08 PubMed PMID: 25376915; PMCID: PMC4302283.
- [11] A. Mariani, S.C. Dowdy, W.A. Cliby, B.S. Gostout, M.B. Jones, T.O. Wilson, K.C. Podratz, Prospective assessment of lymphatic dissemination in endometrial cancer: a paradigm shift in surgical staging, *Gynecol. Oncol.* 109 (1) (2008) 11–18. Epub 2008/02/29 PubMed PMID: 18304622; PMCID: PMC3667391.
- [12] J. Fanning, A. Gangestad, S.J. Andrews, National cancer data base/surveillance epidemiology and end results: potential insensitive-measure bias, *Gynecol. Oncol.* 77 (3) (2000) 450–453. Epub 2000/06/01 PubMed PMID: 10831358.
- [13] K.M. Greven, Tailoring radiation to the extent of disease for uterine-confined endometrial cancer, *Semin. Radiat. Oncol.* 10 (1) (2000) 29–35. Epub 2000/02/15 PubMed PMID: 10671656.
- [14] J.S. Kwon, J.A. Francis, F. Qiu, M.M. Weir, H.C. Ettl, When is a pathology review indicated in endometrial cancer? *Obstet. Gynecol.* 110 (6) (2007) 1224–1230. Epub 2007/12/07 PubMed PMID: 18055713.
- [15] A. Papadia, G. Azioni, B. Brusaca, E. Pulcheri, K. Nishida, S. Menoni, F. Simpkins, J.A. Lucci 3rd, N. Ragni, Frozen section underestimates the need for surgical staging in endometrial cancer patients, *Int. J. Gynecol. Canc. : Off. J. Int. Gynecol. Canc. Soc.* 19 (9) (2009) 1570–1573. Epub 2009/12/04 PubMed PMID: 19955939.
- [16] N. Cancer Genome Atlas Research, C. Kandoth, N. Schultz, A.D. Cherniack, R. Akbani, Y. Liu, H. Shen, A.G. Robertson, I. Pashtan, R. Shen, C.C. Benz, C. Yau, P.W. Laird, L. Ding, W. Zhang, G.B. Mills, R. Kucherlapati, E.R. Mardis, D.A. Levine, Integrated genomic characterization of endometrial carcinoma, *Nature* 497 (7447) (2013) 67–73. PubMed PMID: 23636398; PMCID: PMC3704730.
- [17] S. Bellone, E. Bignotti, S. Lonardi, F. Ferrari, F. Centritto, A. Masserdotti, F. Pettinella, J. Black, G. Menderes, G. Altwerger, P. Hui, S. Lopez, C. de Haydu, E. Bonazzoli, F. Predolini, L. Zammataro, E. Cocco, F. Ferrari, A. Ravaggi, C. Romani, F. Facchetti, E. Sartori, F.E. Odicino, D.A. Silasi, B. Litkouhi, E. Ratner, M. Azodi, P.E. Schwartz, A.D. Santin, Polymerase epsilon (POLE) ultra-mutation in uterine tumors correlates with T lymphocyte infiltration and increased resistance to platinum-based chemotherapy in vitro, *Gynecol. Oncol.* 144 (1) (2017) 146–152. Epub 2016/11/30 PubMed PMID: 27894751; PMCID: PMC5183545.
- [18] S. Bellone, F. Centritto, J. Black, C. Schwab, D. English, E. Cocco, S. Lopez, E. Bonazzoli, F. Predolini, F. Ferrari, D.A. Silasi, E. Ratner, M. Azodi, P.E. Schwartz, A.D. Santin, Polymerase epsilon (POLE) ultra-mutated tumors induce robust tumor-specific CD4+ T cell responses in endometrial cancer patients, *Gynecol. Oncol.* 138 (1) (2015) 11–17. Epub 2015/05/02 PubMed PMID: 25931171; PMCID: 4469551.
- [19] C. Bilbao-Sieyro, R. Ramirez, G. Rodriguez-Gonzalez, O. Falcon, L. Leon, S. Torres, L. Fernandez, S. Alonso, N. Diaz-Chico, M. Perucho, J.C. Diaz-Chico, Microsatellite instability and ploidy status define three categories with distinctive prognostic impact in endometrioid endometrial cancer, *Oncotarget* 5 (15) (2014) 6206–6217. Epub 2014/07/16 PubMed PMID: 25026289; PMCID: PMC4171623.
- [20] P. Gargiulo, C. Della Pepa, S. Berardi, D. Califano, S. Scala, L. Buonaguro, G. Ciliberto, P. Brauchli, S. Pignata, Tumor genotype and immune microenvironment in POLE-ultramutated and MSI-hypermutated Endometrial Cancers: new candidates for checkpoint blockade immunotherapy? *Canc. Treat. Rev.* 48 (2016) 61–68. PubMed PMID: 27362548.
- [21] J.M. Mehnert, A. Panda, H. Zhong, K. Hirshfield, S. Damare, K. Lane, L. Sokol, M.N. Stein, L. Rodriguez-Rodriguez, H.L. Kaufman, S. Ali, J.S. Ross, D.C. Pavlick, G. Bhanot, E.P. White, R.S. DiPaola, A. Lovell, J. Cheng, S. Ganesan, Immune activation and response to pembrolizumab in POLE-mutant endometrial cancer, *J. Clin. Invest.* 126 (6) (2016) 2334–2340. Epub 2016/05/10 PubMed PMID: 27159395; PMCID: PMC4887167.
- [22] J.M. Piulats, E. Guerra, M. Gil-Martin, B. Roman-Canal, S. Gatius, R. Sanz-Pamplona, A. Velasco, A. Vidal, X. Matias-Guiu, Molecular approaches for classifying endometrial carcinoma, *Gynecol. Oncol.* 145 (1) (2017) 200–207. Epub 2017/01/04 PubMed PMID: 28040204.
- [23] I.C. van Gool, F.A. Eggink, L. Freeman-Mills, E. Stelloo, E. Marchi, M. de Bruyn, C. Palles, R.A. Nout, C.D. de Kroon, E.M. Osse, P. Klenerman, C.L. Creutzberg, I.P.M. Tomlinson, V. Smit, H.W. Nijman, T. Bosse, D.N. Church, POLE proofreading mutations elicit an anti-tumor immune response in endometrial cancer, *Clin. Canc. Res. : Off. J. Am. Assoc. Canc. Res.* 21 (14) (2015) 3347–3355. PubMed PMID: 25878334.
- [24] G. Vollmer, Endometrial cancer: experimental models useful for studies on molecular aspects of endometrial cancer and carcinogenesis, *Endocr. Relat. Canc.* 10 (1) (2003) 23–42. Epub 2003/03/26 PubMed PMID: 12653669.
- [25] S. Cabrera, M. Llauro, J. Castellvi, Y. Fernandez, F. Alameda, E. Colas, A. Ruiz, A. Doll, S. Schwartz Jr., R. Carreras, J. Xercavins, M. Abal, A. Gil-Moreno, J. Reventos, Generation and characterization of orthotopic murine models for endometrial cancer, *Clin. Exp. Metastasis* 29 (3) (2012) 217–227. Epub 2011/12/27 PubMed PMID: 22198674.
- [26] I.S. Haldorsen, M. Popa, T. Fønnes, N. Brekke, R. Kopperud, N.C. Visser, C.B. Rygh, T. Pavlin, H.B. Salvesen, E. McCormack, C. Krakstad, Multimodal imaging of orthotopic mouse model of endometrial carcinoma, *PLoS One* 10 (8) (2015), e0135220. Epub 2015/08/08 PubMed PMID: 26252891; PMCID: PMC4529312.
- [27] A. Doll, M. Gonzalez, M. Abal, M. Llauro, M. Rigau, E. Colas, M. Monge, J. Xercavins, G. Capella, B. Diaz, A. Gil-Moreno, F. Alameda, J. Reventos, An orthotopic endometrial cancer mouse model demonstrates a role for RUNX1 in distant metastasis, *Int. J. Canc. J. Int. Canc.* 125 (2) (2009) 257–263. Epub 2009/04/23 PubMed PMID: 19384951.
- [28] J. Depreuw, E. Hermans, S. Schrauwen, D. Annibaldi, L. Coenegrachts, D. Thomas, M. Luycck, I. Gutierrez-Roelens, D. Debruyne, K. Konings, P. Moerman, I. Vergote, D. Lambrechts, F. Amant, Characterization of patient-derived tumor xenograft models of endometrial cancer for preclinical evaluation of targeted therapies, *Gynecol. Oncol.* 139 (1) (2015) 118–126. Epub 2015/08/02 PubMed PMID: 26232337.
- [29] T.H. Kim, H.L. Franco, S.Y. Jung, J. Qin, R.R. Broaddus, J.P. Lydon, J.W. Jeong, The synergistic effect of Mig-6 and Pten ablation on endometrial cancer development and progression, *Oncogene* 29 (26) (2010) 3770–3780. PubMed PMID: 20418913; PMCID: 4013686.
- [30] T.H. Kim, J. Wang, K.Y. Lee, H.L. Franco, R.R. Broaddus, J.P. Lydon, J.W. Jeong, F.J. Demayo, The synergistic effect of conditional pten loss and oncogenic K-ras mutation on endometrial cancer development occurs via decreased progesterone receptor action, *J. Oncol.* 2010 (2010) 139087. Epub 2009/11/04 PubMed PMID: 19884980; PMCID: 2768008.
- [31] T.L. Lu, J.L. Chang, C.C. Liang, L.R. You, C.M. Chen, Tumor spectrum, tumor latency and tumor incidence of the Pten-deficient mice, *PLoS One* 2 (11) (2007) e1237. Epub 2007/11/29 PubMed PMID: 18043744; PMCID: 2077932.
- [32] C.M. Contreras, E.A. Akbay, T.D. Gallardo, J.M. Haynie, S. Sharma, O. Tagao, N. Bardeesy, M. Takahashi, J. Settleman, K.K. Wong, D.H. Castrillon, Lkb1 inactivation is sufficient to drive endometrial cancers that are aggressive yet highly responsive to mTOR inhibitor monotherapy, *Dis. Model. Mech.* 3 (3-4) (2010) 181–193. Epub 2010/02/10 PubMed PMID: 20142330; PMCID: PMC2869492.
- [33] T. Daikoku, Y. Hirota, S. Tranguch, A.R. Joshi, F.J. DeMayo, J.P. Lydon, L.H. Ellenson, S.K. Dey, Conditional loss of uterine Pten unfaithfully and rapidly induces endometrial cancer in mice, *Canc. Res.* 68 (14) (2008) 5619–5627. Epub 2008/07/18 PubMed PMID: 18632614; PMCID: PMC2284329.
- [34] F. Deerberg, J. Kaspareit, Endometrial carcinoma in BD II/Han rats: model of a spontaneous hormone-dependent tumor, *J. Natl. Cancer Inst.* 78 (6) (1987) 1245–1251. Epub 1987/06/01. PubMed PMID: 3473261.
- [35] E. Samuelson, C. Hedberg, S. Nilsson, A. Behndorf, Molecular classification of spontaneous endometrial adenocarcinomas in BDII rats, *Endocr. Relat. Canc.* 16 (1) (2009) 99–111. Epub 2008/12/17 PubMed PMID: 19075038.
- [36] H. Cheng, P. Liu, F. Zhang, E. Xu, L. Symonds, C.E. Ohlson, R.T. Bronson, S.M. Maira, E. Di Tomaso, J. Li, A.P. Myers, L.C. Cantley, G.B. Mills, J.J. Zhao, A genetic mouse model of invasive endometrial cancer driven by concurrent loss of Pten and Lkb1 is highly responsive to mTOR inhibition, *Canc. Res.* 74 (1) (2014) 15–23. Epub 2013/12/11 PubMed PMID: 24322983; PMCID: 3982380.
- [37] Y. Gao, P. Lin, J.P. Lydon, Q. Li, Conditional abrogation of transforming growth factor-beta receptor 1 in PTEN-inactivated endometrium promotes endometrial cancer progression in mice, *J. Pathol.* 243 (1) (2017) 89–99. Epub 2017/06/29 PubMed PMID: 28657664; PMCID: PMC5568928.
- [38] P.A. Steck, M.A. Pershouse, S.A. Jasser, W.K. Yung, H. Lin, A.H. Ligon, L.A. Langford, M.L. Baumgard, T. Hattier, T. Davis, C. Frye, R. Hu, B. Swedlund, D.H. Teng, S.V. Tavtigian, Identification of a candidate tumour suppressor gene, MMAC1, at chromosome 10q23.3 that is mutated in multiple advanced cancers, *Nat. Genet.* 15 (4) (1997) 356–362. Epub 1997/04/01 PubMed PMID: 9090379.
- [39] D.M. Li, H. Sun, TEPI, encoded by a candidate tumor suppressor locus, is a novel protein tyrosine phosphatase regulated by transforming growth factor beta, *Canc. Res.* 57 (11) (1997) 2124–2129. Epub 1997/06/01. PubMed PMID: 9187108.
- [40] J.I. Risinger, K. Hayes, G.L. Maxwell, M.E. Carney, R.K. Dodge, J.C. Barrett, A. Berchuck, PTEN mutation in endometrial cancers is associated with favorable clinical and pathologic characteristics, *Clin. Canc. Res.* 4 (12) (1998) 3005–3010. PubMed PMID: 9865913.
- [41] G.L. Maxwell, J.I. Risinger, C. Gumbs, H. Shaw, R.C. Bentley, J.C. Barrett, A. Berchuck, P.A. Futreal, Mutation of the PTEN tumor suppressor gene in endometrial hyperplasias, *Canc. Res.* 58 (12) (1998) 2500–2503. PubMed PMID: 9635567.
- [42] A. Di Cristofano, L.H. Ellenson, Endometrial carcinoma, *Ann. Rev. Pathol.* 2 (2007) 57–85. Epub 2007/11/28 PubMed PMID: 18039093.
- [43] A. Miyasaka, K. Oda, Y. Ikeda, K. Sone, T. Fukuda, K. Inaba, C. Makii, A. Enomoto, N. Hosoya, M. Tanikawa, Y. Uehara, T. Arimoto, H. Kuramoto, O. Wada-Hiraike, K. Miyaogawa, T. Yano, K. Kawana, Y. Osuga, T. Fujii, PI3K/mTOR pathway inhibition overcomes radioresistance via suppression of the HIF1-alpha/VEGF pathway in endometrial cancer, *Gynecol. Oncol.* 138 (1) (2015) 174–180. Epub 2015/04/29 PubMed PMID: 25913131.
- [44] A.J. Shorthouse, J.F. Smyth, G.G. Steel, M. Ellison, J. Mills, M.J. Peckham, The human tumour xenograft—a valid model in experimental chemotherapy? *Br. J. Surg.* 67 (10) (1980) 715–722. Epub 1980/10/01. PubMed PMID: 6253000.
- [45] J.J. Tentler, A.C. Tan, C.D. Weekes, A. Jimeno, S. Leong, T.M. Pitts, J.J. Arcaroli, W.A. Messersmith, S.G. Eckhardt, Patient-derived tumour xenografts as models for oncology drug development, *Nat. Rev. Clin. Oncol.* 9 (6) (2012) 338–350. Epub 2012/04/18 PubMed PMID: 22508028; PMCID: PMC3928688.
- [46] M. Hidalgo, F. Amant, A.V. Biankin, E. Budinska, A.T. Byrne, C. Caldas, R.B. Clarke, S. de Jong, J. Jonkers, G.M. Maelandsmo, S. Roman-Roman, J. Seoane, L. Trusolino, A. Villanueva, Patient-derived xenograft models: an emerging platform for

- translational cancer research, *Canc. Discov.* 4 (9) (2014) 998–1013. Epub 2014/09/04 PubMed PMID: 25185190; PMCID: PMC4167608.
- [47] M.H. Tan, T.M. Chu, Characterization of the tumorigenic and metastatic properties of a human pancreatic tumor cell line (AsPC-1) implanted orthotopically into nude mice, *Tum. Biol. : J. Int. Soc. Oncodevelop. Biol. Med.* 6 (1) (1985) 89–98. Epub 1985/01/01. PubMed PMID: 4023565.
- [48] C. Merenda, B. Sordat, J.P. Mach, S. Carrel, Human endometrial carcinomas serially transplanted in nude mice and established in continuous cell lines, *Int. J. Canc. J. Int. Canc.* 16 (4) (1975) 559–570. Epub 1975/10/15. PubMed PMID: 1176207.
- [49] J. Rygaard, C.O. Povlsen, Heterotransplantation of a human malignant tumour to "Nude" mice, *Acta Pathol. Microbiol. Scand.* 77 (4) (1969) 758–760. Epub 1969/01/01. PubMed PMID: 5383844.
- [50] J.E. Palm, M.N. Teller, P.C. Merker, G.W. Woolley, Host conditioning in experimental chemotherapy, *Ann. N. Y. Acad. Sci.* 76 (3) (1958) 812–820. Epub 1958/12/05. PubMed PMID: 13627908.
- [51] K. Unno, M. Ono, A.D. Winder, K.P. Maniar, A.S. Paintal, Y. Yu, J.J. Wei, J.R. Lurain, J.J. Kim, Establishment of human patient-derived endometrial cancer xenografts in NOD scid gamma mice for the study of invasion and metastasis, *PLoS One* 9 (12) (2014), e116064. Epub 2014/12/30 PubMed PMID: 25542024; PMCID: PMC4277433.
- [52] M. Nakamura, S. Kyo, B. Zhang, X. Zhang, Y. Mizumoto, M. Takakura, Y. Maida, N. Mori, M. Hashimoto, S. Ohno, M. Inoue, Prognostic impact of CD133 expression as a tumor-initiating cell marker in endometrial cancer, *Hum. Pathol.* 41 (11) (2010) 1516–1529. Epub 2010/08/31 PubMed PMID: 20800872.
- [53] S. Rutella, G. Bonanno, A. Procoli, A. Mariotti, M. Corallo, M.G. Prisco, A. Eramo, C. Napoletano, D. Gallo, A. Perillo, M. Nuti, L. Pierelli, U. Testa, G. Scambia, G. Ferrandina, Cells with characteristics of cancer stem/progenitor cells express the CD133 antigen in human endometrial tumors, *Clin. Canc. Res.* 15 (13) (2009) 4299–4311. Epub 2009/06/11 PubMed PMID: 19509143.
- [54] A. Zehir, R. Benayed, R.H. Shah, A. Syed, S. Middha, H.R. Kim, P. Srinivasan, J. Gao, D. Chakravarty, S.M. Devlin, M.D. Hellmann, D.A. Barron, A.M. Schram, M. Hameed, S. Dogan, D.S. Ross, J.F. Hechtman, D.F. DeLair, J. Yao, D.L. Mandelker, D.T. Cheng, R. Chandramohan, A.S. Mohanty, R.N. Ptashkin, G. Jayakumar, M. Prasad, M.H. Syed, A.B. Rema, Z.Y. Liu, K. Nafa, L. Borsu, J. Sadowska, J. Casanova, R. Bacaes, L.J. Kiecka, A. Razumova, J.B. Son, L. Stewart, T. Baldi, K.A. Mullaney, H. Al-Ahmadie, E. Vakiani, A.A. Abeshouse, A.V. Penson, P. Jonsson, N. Camacho, M.T. Chang, H.H. Won, B.E. Gross, R. Kundra, Z.J. Heins, H.W. Chen, S. Phillips, H. Zhang, J. Wang, A. Ochoa, J. Wills, M. Eubank, S.B. Thomas, S.M. Gardos, D.N. Reales, J. Galle, R. Durany, R. Cambria, W. Abida, A. Cercek, D.R. Feldman, M.M. Gounder, A.A. Hakimi, J.J. Harding, G. Iyer, Y.Y. Janjigian, E.J. Jordan, C.M. Kelly, M.A. Lowery, L.G.T. Morris, A.M. Omuro, N. Raj, P. Razavi, A.N. Shoushtari, N. Shukla, T.E. Soumerai, A.M. Varghese, R. Yaeger, J. Coleman, B. Bochner, G.J. Riely, L.B. Saltz, H.I. Scher, P.J. Sabbatini, M.E. Robson, D.S. Klimstra, B.S. Taylor, J. Baselga, N. Schultz, D.M. Hyman, M.E. Arcila, D.B. Solit, M. Ladanyi, M.F. Berger, Mutational landscape of metastatic cancer revealed from prospective clinical sequencing of 10,000 patients, *Nat. Med.* 23 (6) (2017) 703–713. Epub 2017/05/10 PubMed PMID: 28481359; PMCID: PMC5461196.
- [55] M. Iijima, K. Banno, R. Okawa, M. Yanokura, M. Iida, T. Takeda, H. Kunitomi-Irie, M. Adachi, K. Nakamura, K. Umene, Y. Nogami, K. Masuda, E. Tominaga, D. Aoki, Genome-wide analysis of gynecologic cancer: the Cancer Genome Atlas in ovarian and endometrial cancer, *Oncol. Lett.* 13 (3) (2017) 1063–1070. Epub 2017/04/30 PubMed PMID: 28454214; PMCID: PMC5403284.
- [56] A.M. Kamal, J.N. Bulmer, S.B. DeCruze, H.F. Stringfellow, P. Martin-Hirsch, D.K. Hapangama, Androgen receptors are acquired by healthy postmenopausal endometrial epithelium and their subsequent loss in endometrial cancer is associated with poor survival, *Br. J. Canc.* 114 (6) (2016) 688–696. Epub 2016/03/02 PubMed PMID: 26930451; PMCID: PMC4800292.
- [57] R. Vihko, A. Alanko, V. Isomaa, A. Kauppila, The predictive value of steroid hormone receptor analysis in breast, endometrial and ovarian cancer, *Med. Oncol. Tumor Pharmacother.* 3 (3-4) (1986) 197–210. Epub 1986/01/01. PubMed PMID: 3543533.
- [58] N. Saito, [Biochemical analysis of estrogen receptor and progesterone receptor in normal uterus and endometrial carcinoma], *Nihon Naibunpi Gakkai zasshi* 63 (2) (1987) 87–101. Epub 1987/02/20. PubMed PMID: 3569607.
- [59] D. Tomica, S. Ramic, D. Danolic, L. Susnjar, M. Peric-Balja, M. Puljiz, Impact of oestrogen and progesterone receptor expression in the cancer cells and myometrium on survival of patients with endometrial cancer, *J. Obstet. Gynaecol. : J. Instit. Obstetr. Gynaecol.* (2017) 1–7. Epub 2017/08/03 PubMed PMID: 28764605.
- [60] M. Singh, R.J. Zaino, V.J. Filiaci, K.K. Leslie, Relationship of estrogen and progesterone receptors to clinical outcome in metastatic endometrial carcinoma: a Gynecologic Oncology Group Study, *Gynecol. Oncol.* 106 (2) (2007) 325–333. Epub 2007/05/29 PubMed PMID: 17532033.
- [61] R.C. Burghardt, P.A. Mitchell, R. Kurten, Gap junction modulation in rat uterus. II. Effects of antiestrogens on myometrial and serosal cells, *Biol. Reprod.* 30 (1) (1984) 249–255. Epub 1984/02/01. PubMed PMID: 6421335.
- [62] R. Zeng, X. Li, G.I. Gorodeski, Estrogen abrogates transcervical tight junctional resistance by acceleration of occludin modulation, *J. Clin. Endocrinol. Metabol.* 89 (10) (2004) 5145–5155. Epub 2004/10/09 PubMed PMID: 15472219.
- [63] G.I. Gorodeski, Estrogen modulation of epithelial permeability in cervical-vaginal cells of premenopausal and postmenopausal women, *Menopause* 14 (6) (2007) 1012–1019. Epub 2007/06/19 PubMed PMID: 17572644; PMCID: PMC2366810.
- [64] M.A. Herve, G. Meduri, F.G. Petit, T.S. Domet, G. Lazenec, S. Mourah, M. Perrot-Appianat, Regulation of the vascular endothelial growth factor (VEGF) receptor Flk-1/KDR by estradiol through VEGF in uterus, *J. Endocrinol.* 188 (1) (2006) 91–99. Epub 2006/01/06 PubMed PMID: 16394178.
- [65] J. Liu, Y. Liu, W. Wang, C. Wang, Y. Che, Expression of immune checkpoint molecules in endometrial carcinoma, *Exp. Ther. Med.* 10 (5) (2015) 1947–1952. Epub 2015/12/08 PubMed PMID: 26640578; PMCID: PMC4665362.
- [66] N.L. Jones, J. Xiu, S.K. Reddy, W.M. Burke, A.I. Tergas, J.D. Wright, J.Y. Hou, Identification of potential therapeutic targets by molecular profiling of 628 cases of uterine serous carcinoma, *Gynecol. Oncol.* 138 (3) (2015) 620–626. Epub 2015/07/01 PubMed PMID: 26123645.
- [67] M.E. Urick, M.L. Rudd, A.K. Godwin, D. Sgroi, M. Merino, D.W. Bell, PIK3R1 (p85alpha) is somatically mutated at high frequency in primary endometrial cancer, *Canc. Res.* 71 (12) (2011) 4061–4067. Epub 2011/04/12 PubMed PMID: 21478295; PMCID: 3117071.
- [68] J. Greenaway, R. Moorehead, P. Shaw, J. Petrik, Epithelial-stromal interaction increases cell proliferation, survival and tumorigenicity in a mouse model of human epithelial ovarian cancer, *Gynecol. Oncol.* 108 (2) (2008) 385–394. Epub 2007/11/27 PubMed PMID: 18036641.
- [69] G. Vollmer, M.R. Schneider, The rat endometrial adenocarcinoma cell line RUCA-1: a novel hormone-responsive *in vivo/in vitro* tumor model, *J. Steroid Biochem. Mol. Biol.* 58 (1) (1996) 103–115. Epub 1996/04/01 PubMed PMID: 8809192.